Nanostructure and grain size characterization in $Al_{84}Si_6Cu_3Mg_7$ ribbons and ingots

I. Alfonso and G. González
Instituto de Investigaciones en Materiales, Universidad Nacional Autónoma de México, Circuito Exterior, Cd. Universitaria, Del. Coyoacán, México, DF. 04510, México, Tel. 52 55 56224502, e-mail: ialfonso@iim.unam.mx

C. Maldonado and A. Medina
Instituto de Investigaciones Metalúrgicas, Universidad Michoacana de San Nicolás de Hidalgo, Morelia, Mich. 58000, México.

L. Bejar
Facultad de Ingeniería Mecánica, Universidad Michoacana de San Nicolás de Hidalgo, Morelia, Mich. 58000, México.

Recibido el 8 de septiembre de 2008; aceptado el 8 de diciembre de 2008

An $Al_{84}Si_6Cu_3Mg_7$ alloy was produced by melt-spun and conventional casting and characterized using X-Ray Diffractometry (XRD), Scanning Electron Microscopy (SEM), High Resolution Transmission Electron Microscopy (HRTEM) and microhardness techniques. Melt-spun minimizes second phase formation and increases the alloying content in solid solution. Q phase ($Al_5Cu_2Mg_8Si_6$) nanocrystallites (5 nm) were observed for melt-spun alloys. The high alloying content in solid solution and the small α-Al grain size (300 nm) for ribbons lead to a hardness improvement of about 2.4 times greater than that of conventionally cast alloys.

Keywords: Melt-spun; aluminum alloys; magnesium; nanostructure; superstructure.

Se fabricó una aleación cuaternaria $Al_{84}Si_6Cu_3Mg_7$ utilizando melt-spun y fundición convencional, la cual se caracterizó mediante Difracción de Rayos-X, Microscopía Electrónica de Barrido y de Transmisión de Alta Resolución y Microdureza. El uso del melt-spun llevó a la disminución de la formación de segundas fases e incrementó el contenido de elementos de aleación en solución sólida. En las aleaciones obtenidas por melt-spun se observaron nanocristales de 5 nm de la fase Q ($Al_5Cu_2Mg_8Si_6$). El alto contenido de elementos de aleación en solución sólida y el pequeño tamaño de los granos de α-Al (300 nm) provocó que para las cintas la dureza fuera cerca de 2.4 veces mayor que la dureza de las aleaciones obtenidas por fundición convencional.

Descriptores: Melt-spun; aleaciones de aluminio; magnesio; nanoestructura; superestructura.

PACS: 61.46.+w; 81.16.-c; 68.37.Lp; 81.07.-b

1. Introduction

One common material for automotive industry applications is the Al-Si-Cu-Mg 319 alloy. This alloy has good castability, excellent corrosion resistance and machinability, medium strength, and low specific weight. Its silicon content ranges from 5.5 to 6.5 (wt.%), and copper varies from 3.0 to 4.0 (wt.%). The presence of magnesium improves strain, hardenability and improves the material strength [1]. The as-cast structure for Al-Si-Cu-Mg alloys includesα-Al, Si eutectic particles, Mg_2Si, Al_2Cu, $Al_5Cu_2Mg_8Si_6$ [1,2]. There are few published works about conventional casting and heat treatment of this alloy [1,2]. For further application, it is necessary to develop new high performance alloys or casting processes. From previous investigations for other Al alloy systems [3-5], it has been shown that alloys obtained by rapid solidification processes (RSP) reveal outstanding mechanical properties. Applying a RSP it is possible to avoid or minimize second phases formation, and obtain a supersaturated solid solution with a higher quantity of alloying elements, allowing to form metastable crystalline, nanocrystalline and amorphous phases, strengthening the alloys [3-5]. Q phase plays a key role in controlling the properties in these alloys because of its widespread and often dominant presence [6]. Yet, historically Q did not receive the systematic studies for its influence on properties as did some of other phases [6]. In recent years, however, several studies reported interesting results. Our previous studies [7,8] for Al-Si-Cu-Mg melt-spun ribbons report Q phase formation when Mg content increased. In the present work we intend to gain further insight by providing information about Q phase structure. The presence of Q phase as a superstructure, for heat treated Al-Cu-Mg alloys with Si additions, has been reported by Cayron and Buffat [9]. For as-cast Al-Si-Cu-Mg alloys superstructures formation has not reported. The rapid solidification reached using melt-spun allows freezing a high vacancies concentration. One of the hypotheses of this work is that applying an RSP it is also possible to produce superstructures in Al-Si-Cu-Mg alloys. Therefore it is necessary to study grain size decrease and the possible formation of superstructures and other structures or phases, characteristics of RSP which lead to the alloys strengthening. In this work nanostructure and

TABLE I. Average chemical composition (wt.%) of the experimental alloy.

Si	Cu	Mg	Fe	Mn	Zn	Ti	Al
5.84	2.95	6.78	0.31	0.07	0.03	0.12	Balance

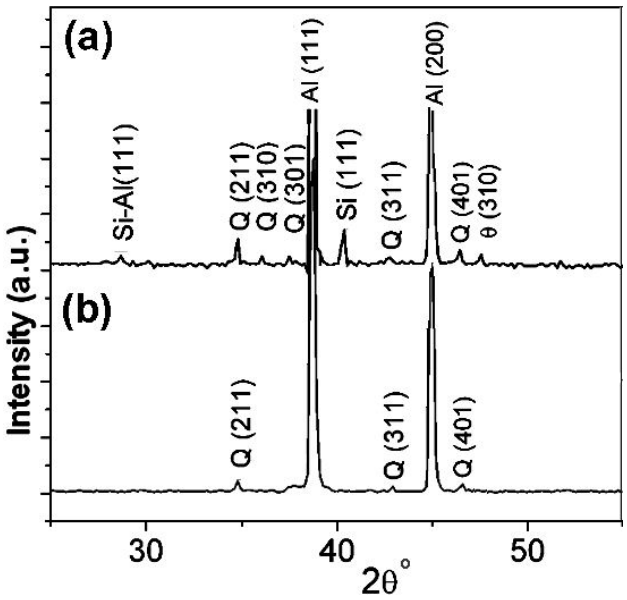

FIGURE 1. (a) X-ray diffraction patterns taken from $Al_{84}Si_6Cu_3Mg_7$ conventionally cast alloys, and (b) from the wheel side surface of rapidly solidified alloys. As can be observed second phases formation was minimized for melt-spun ribbons.

microhardness for the modified 319 alloy are dealt with by examining melt-spun ribbons using XRD, SEM and HRTEM.

2. Experimental

A 356 alloy ingot, with Al-8.5Si-0.3Mg (wt.%) was used as master alloy. Pure Cu (powder, $> 99.99\%$ purity) and Mg (ingot, $> 99.95\%$ purity) were added to control the alloying content. Castings were carried out in graphite crucibles using an induction furnace under a controlled Ar atmosphere. Obtained ingots were then remolten in a quartz tube and ejected through a 0.5 mm diameter hole on to the surface of a polished copper wheel with a diameter of 200 mm. The experiments were carried out under a helium atmosphere to avoid melt oxidation. The ribbons were produced with a rotating speed of 40 ms^{-1}. Table I shows the chemical composition of the experimental alloys.

Experimental alloys were characterized using TEM, XRD and microhardness techniques. XRD measurements were carried out in a Siemens 400 X-ray diffractometer using CuKα radiation at 30 k and 25 mA. SEM was carried out in a JEOL JSM 6400 operated at 20 kV. TEM and HRTEM investigations were conducted using a FEG-Philips Tecnai F20 transmission electron microscope operated at 200 kV, with an energy dispersive X-ray spectroscopy (EDX) attachment (nano EDX with a 3 nm in diameter spot size). Specimens for TEM were prepared by dimpling using a Gatan 656 Dimple Grinder followed by Argon ions milling using a Gatan 691 Precision Ion Polishing System (PIPS). Microhardness measurements were made with a Vickers diamond indenter in a Leitz Wetzlar microhardness tester employing a load of 25 g for 15 s.

3. Results and discussion

Figures 1a and 1b show XRD patterns taken from conventionally cast alloys and from melt-spun ribbons, respectively. A representative range is shown for 2θ (from 25 to 55), making possible to remark the differences between the alloys. Evidence in Fig. 1b suggests limited solid solution and minimized second phase formation for ribbons. Whereas diffrac-

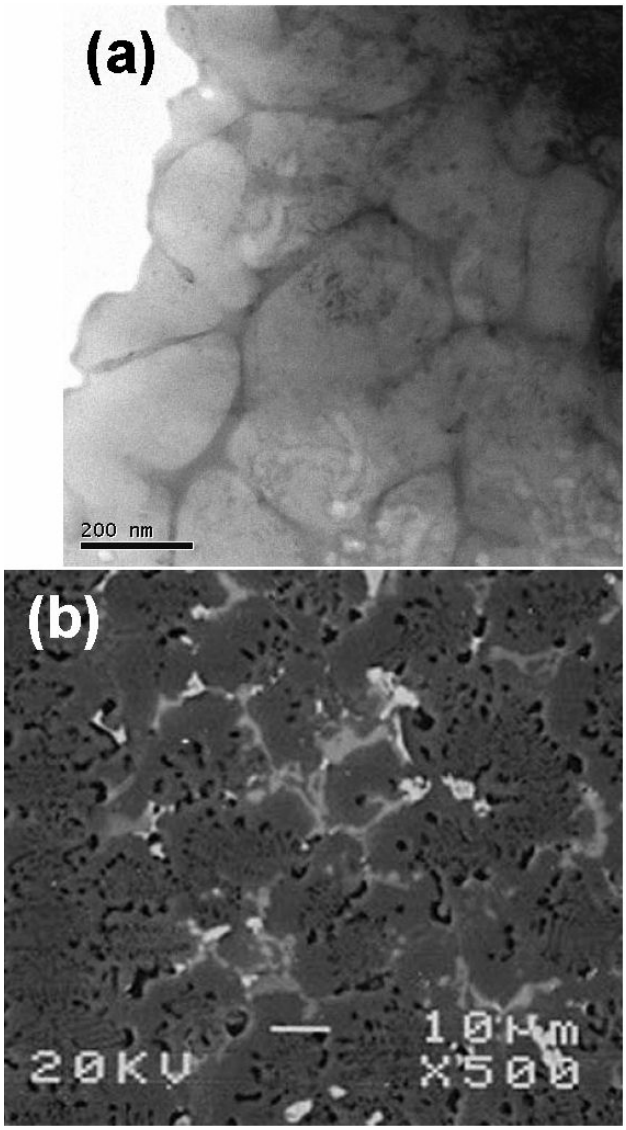

FIGURE 2. (a) Bright field TEM image for melt-spun ribbons and (b) SEM image for ingots. 300 - 400 nm and 20-30 mm α-Al cells can be observed for ribbons and ingots respectively.

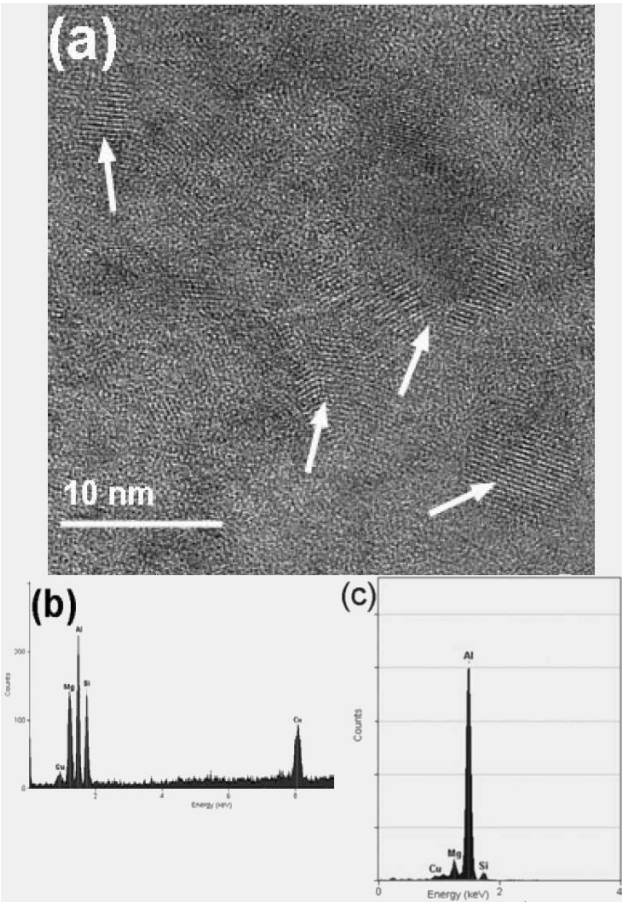

FIGURE 3. (a) HRTEM micrograph of melt-spun ribbons showing the presence of nanocrystallites, (b) EDX of the nanoparticles and (c) EDX of the interparticle zone.

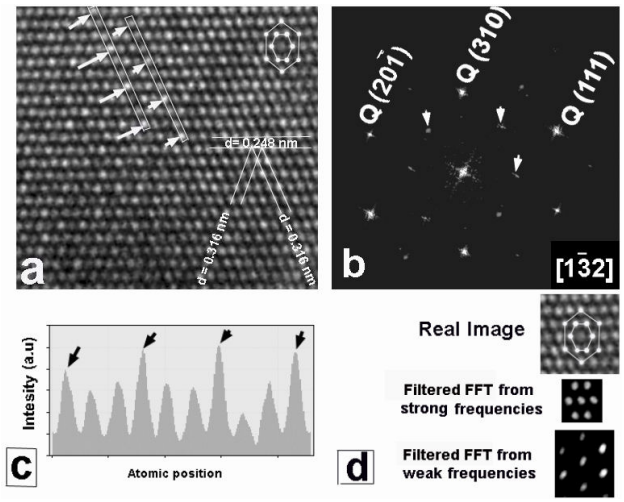

FIGURE 4. (a) HRTEM micrograph corresponding to Q phase. One can see the periodical distribution of the brightest spots (arrowed), mainly attributed to the superstructure modulation. (b) FFT showing the main frequencies corresponding to Q phase and the superstructure (arrowed). (c) An intensity profile along the atomic layer outlined by solid lines, further revealing the modulation of the contrast. (d) Comparison between real image and filtered FFT.

tion peaks belonging to the α-Al, Si, Al-Si eutectic, Q and θ (Al_2Cu) phases are present in the conventionally cast alloy, only diffraction peaks belonging to Al solid solution and Q phase are present for ribbons. No efforts were made to get full solubility because it is not relevant for our objectives, besides formation of fine dispersions of high-modulus second-phase particles increases strength, wear resistance and thermal stability [4]. Despite limited solid solubility, RSP also led to high concentration of alloying elements in the supersaturated solid solution. Whereas for melt-spun ribbons Si and Mg average atomic percents were 4.4 and 6.7, respectively, for the conventionally cast alloys this values only reach 0.3 and 0.1 Minimize second phase formation and enough solid solubility of alloying elements in α-Al matrix because rapid solidification has been extensively reported [3-5,10].

SEM and TEM techniques were applied to further study α-Al grain size and second phases. Figure 2a shows grain size refining for melt-spun alloys. Equiaxed fine grains with grain sizes of 300 - 400 nm for the Al matrix can be observed for ribbons, while grain size for ingots are 20 - 30 μm. For melt spun ribbons reported grain sizes are between 100 and 500 nm [11,12]. The small α-Al cell size and the high alloying elements concentration in the supersaturated solid solution govern melt-spun ribbons strengthening [13]. Microhardness values for the experimental ribbons (211.7 ± 6.3 kg/mm^2) were more than 2.4 times greater than the microhardness for similar alloys obtained by conventional casting (87.6 ± 2.0 kg/mm^2).

HRTEM and nanobeam EDX (3 nm spot size) were used to analyze the presence of Q nanoparticles. Figure 3a shows a nanostructure composed by well-defined 5 nm particles (arrowed) surrounded by fcc-Al. The EDX profile observed in Fig. 3b shows Al, Si, Cu and Mg signals. Al:Cu:Mg:Si ratios close to $Al_5Cu_2Mg_8Si_6$ show that nanoparticles match to Q phase. This composition is consistent with XRD results. EDX profiles (Fig. 3c) taken from interparticle regions confirmed that it corresponds to α-Al. The volume fraction of Q phase determined by the image analyzer was about 20%. The crystal orientation of each particle appears to be fully random, despite the small interparticle distance lower than 10 nm. No coherent particles-α-Al interphases were observed. Nanoparticles contribution in hardness improvement is also important because of Orowan mechanism [4,14].

Figure 4a is an HRTEM micrograph corresponding to Q phase. It is found that Q phase display a crystal structure different from Q phase observed in as-cast conventionally cast alloys. The Fast Fourier Transformed (FFT) of the image is observed in Fig. 4b, which shows frequencies with strong intensities corresponding to [1-3,2] zone axis of Q hexagonal cell. However, some weak frequencies are also seen in the FFT (arrowed) and could be credited to an incommensurate superlattice. From HRTEM image in Fig. 4a one can see the periodical distribution of the arrowed brightest spots, mainly attributed to the superstructure modulation. The small and big quasi-hexagons represent Q phase and the superstructure. An intensity profile along the atomic layer outlined by

white solid lines see Fig. 4a is shown in Fig. 4c and reveals the modulation of the contrast. Fig. 4d shows real and filtered images obtained using masking tools (Gatan Digital MicrographTM 3.7.0) for strong and weak frequencies from FFT shown in Fig. 4c. As can be observed filtered images are in correspondence with the real image. Incommensurate superlattices are often originated because of periodic shifts respect to the fundamental lattice or periodical changes in compositions or atomic positions [15]. Such superstructures have not been reported in literature for as-cast quaternary Al-Si-Cu-Mg alloys and its presence is assumed to be other of the causes of the high microhardness for these alloys [16]. Unfortunately, because of the small particle sizes, it was not possible to find others zone axis showing similar modulation features. Studies of Q phase superstructure are in progress.

4. Conclusions

From the analysis of the results, it can be concluded that melt-spun allowed minimize second phases formation and increase solid solubility Observed second phases were Q ($Al_5Cu_2Mg_8Si_6$) for melt-spun ribbons and Si, Al-Si eutectic, Q and θ (Al_2Cu) for conventionally cast alloys. Nanostructure for rapid solidified alloys was composed for well-defined 5 nm Q nanoparticles surrounded by fcc α-Al, with grain size between 300 - 400 nm. A superlattice was found for Q nanoparticles. Melt-spun ribbons presented a microhardness improvement of about 2.4 times than that of the conventionally cast alloys with the same composition, mainly originated from the high alloying elements concentration in the supersaturated solid solution and from the small α-Al cell size.

Acknowledgements

The authors are thankful to F. Solorio and R.D. Cervantes from IIM-UMSNH and G. Lara from IIM-UNAM, México, for technical support.

1. P. Ouellet and F.H. Samuel, *Journal of Materials Science* **34** (1999) 4671.
2. F.H. Samuel, A.M. Samuel, and H. Liu, *Journal of Materials Science* **30** (1995) 2531.
3. A. Inoue, Y. Horio, Y.H. Kim, and T. Masumoto, *Materials Transactions* **33** (1992) 669.
4. M. Lutfi, Ovecoglu, N.O. Unlu, N. Eruslu, and E. Genc, *Materials Letters* **57** (2003) 296.
5. T. Nakano, A. Negishi, K. Hayashi, and Y. Umakoshi, *Acta Materialia* **47** (1999) 1091.
6. D.J. Chakrabarti, B.K. Cheong, and D.E. Laughlin, *Proc. TMS Annual Meeting in San Antonio*, (TX, ed. Subodh K. Das, TMS, Warrendale, 1998) p. 27.
7. I. Alfonso *et al.*, *Materials Characterization* **58** (2007) 509.
8. I. Alfonso, C. Maldonado, G. Gonzálezs, A. Medina, and L. Béjar, *Advances in Technology of Materials and Materials Processing Journal* **8** (2006) 196.
9. C. Cayron and P.A. Buffat, *Acta Materialia* **48** (2000) 2639.
10. F.J. Dom, *Aluminium* **70** (1994) 577.
11. K. Ohtera, A. Inoue, T. Terabayashi, H. Nagahama, and T. Musumoto, *Materials Transactions* **33** (1992) 775.
12. M.J. Kramer, L.H. Lewis, Y. Tang, K.W. Dennis, and R.W. McCallum, *Scripta Materialia* **47** (2002) 557.
13. Y. Wang, Z. Zhang, W. Wang, and X. Bian, *Materials Science and Engineering A* **366** (2004) 17.
14. Y.H. Kim, A. Inoue and T. Masumoto, *Materials Transactions* **32** (1991) 599.
15. X.J. Wu *et al.*, *Physica C* **247** (1995) 102.
16. M.D. Bentzon, J.V. Wonterghem, S. Morup, A. Thoelen and C.J. Koch, *Philosophical Magazine B* **60** (1989) 169.